Figure S1

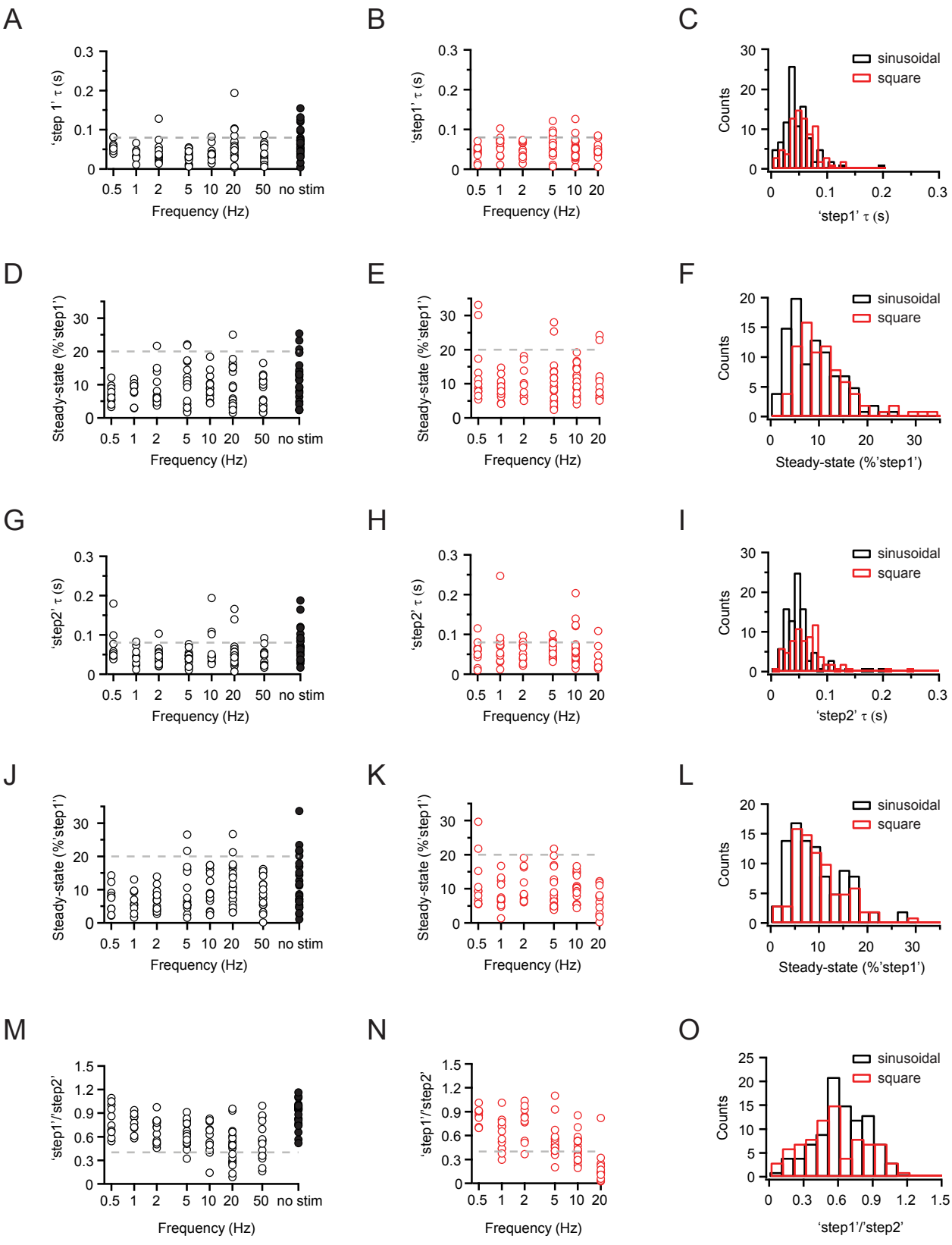
A
B
C
D
E
F
G
H
I
J
K
L
M
N
O
'step 1' τ (s)
'step1' τ (s)
'step2' τ (s)
Steady-state (%'step1')
'step1'/'step2'
Frequency (Hz)
0.5 1 2 5 10 20 50 no stim
0.5 1 2 5 10 20
Counts
sinusoidal
square
'step1' τ (s)
Steady-state (%'step1')
'step2' τ (s)
'step1'/'step2'

Figure S1. Criteria used for triaging cell-attached recordings. Related to Figures 1, 2, and 3.

(A) Inactivation time constant τ for '*step1*', from a double-exponential fit (see Methods) from sinusoidal pressure-clamp stimulations as a function of stimulus frequency, and from experiments without repetitive stimulation ('no stim'). Cells with τ> 0.08 s (dashed gray line) were excluded from further analysis. (B) Inactivation time constant τ (from a double-exponential fit to the activating and inactivating current (Wu et al., 2016)) for '*step1*' from square pulse experiments. Cells with τ> 0.08 s (dashed gray line) were excluded from further analysis. (C) Histogram of distribution of '*pulse1*' time constant τ from sinusoidal (black) and square pulse (red) experiments. Bin size is 10 ms. (D) Steady-state current (calculated as mean current over the last 10 ms of a 300 ms stimulus) for '*step1*' from sinusoidal experiments and experiments without repetitive stimulation ('*no stim*'). Cells with steady-state current > 20% (dashed gray line) were excluded from further analysis. (E) Steady-state current for '*step1*' from square pulse experiments. Cells with steady-state current >20% (dashed gray line) were excluded from further analysis. (F) Histogram of distribution of steady-state currents from sinusoidal (black) and square pulse (red) experiments. Bin size is 2%. (G-I) Same as A-C, for '*step2*'. (J-L) Same as D-F, for '*step2*'. (M) Ratio of peak amplitudes of '*step1*' and '*step2*' for sinusoidal pressure-clamp stimulations and from experiments without repetitive stimulation ('*no stim*'). Cells with a ratio <0.40 (dashed gray line) were excluded from further analysis, which is justified by the upper limit on time constant of recovery from inactivation we observed (10.2 s), which predicts only ~63% recovery after a 10 s rest period. (N) Ratio of peak amplitudes of '*step1*' and '*step2*' from square pulse experiments. Cells with a ratio <0.40 (dashed gray line) were excluded from further analysis. (O) Histogram of distribution of peak amplitude ratios from sinusoidal (black) and square pulse (red) experiments. Bin size is 0.1. After triaging for sinusoidal stimulus (cells excluded/total cells): 0.5 Hz (2/10); 1 Hz (1/9); 2 Hz (2/14); 5 Hz (3/16); 10 Hz (3/12); 20 Hz (11/20); 50 Hz (6/15). After triaging for square stimulus (cells excluded/total cells): 0.5 Hz (3/11); 1 Hz (5/12); 2 Hz (3/10); 5 Hz (5/16); 10 Hz (13/20); 20 Hz (11/12).

Figure S2

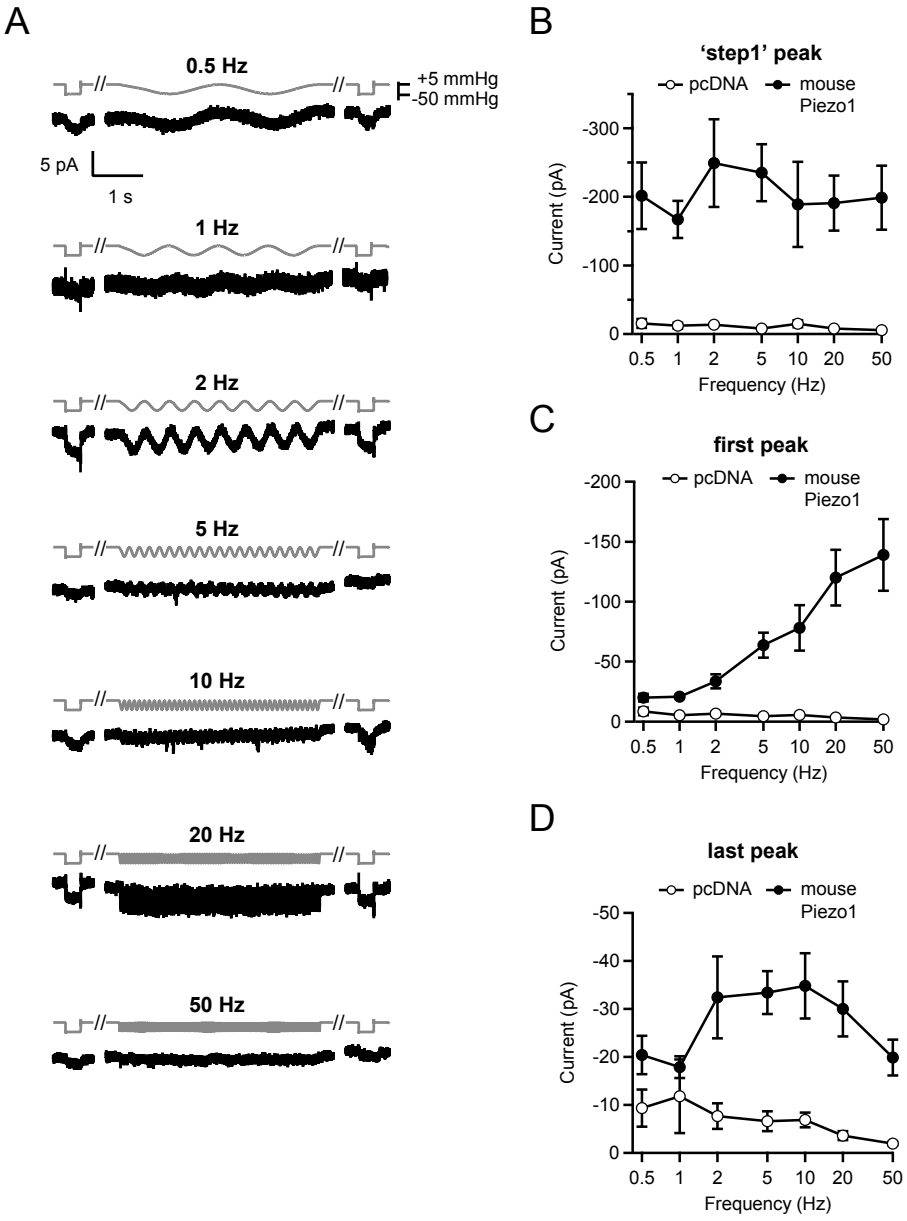
A
0.5 Hz
+5 mmHg
-50 mmHg
P
5 pA
1 s
1 Hz
2 Hz
5 Hz
10 Hz
20 Hz
50 Hz
B
'step1' peak
pcDNA
mouse Piezo1
Current (pA)
-300
-200
-100
0
0.5 1 2 5 10 20 50
Frequency (Hz)
C
first peak
pcDNA
mouse Piezo1
Current (pA)
-200
-150
-100
-50
0
0.5 1 2 5 10 20 50
Frequency (Hz)
D
last peak
pcDNA
mouse Piezo1
Current (pA)
-50
-40
-30
-20
-10
0
0.5 1 2 5 10 20 50
Frequency (Hz)

Figure S2: Currents induced by sinusoidal pressure stimuli are Piezo1-dependent. Related to Figure 1.

(A) Stimulus protocols and representative raw currents from cell-attached patches from HEK293t cells expressing empty vector (pcDNA3.1(+)) and GFP. Each current trace originates from a separate cell-attached patch. (B) Mean peak current amplitude of '*step1*' for HEK293t cells expressing mouse Piezo1 (N = 8-13 cells per stimulation frequency; see **Figure 1**) or pcDNA (N = 6 cells per stimulation frequency). (C) Mean amplitude of '*first peak*' current elicited by the sinusoidal stimulus for HEK293t cells transiently transfected with mouse Piezo1 (N = 8-13 cells per stimulation frequency) or pcDNA (N = 6 cells per stimulation frequency). (D) Mean amplitude of '*last peak*' current elicited by the sinusoidal stimulus for HEK293t cells transiently transfected with mouse Piezo1 (N = 8-13 cells per stimulation frequency) or pcDNA (N = 6 cells per stimulation frequency). All data are mean ± s.e.m.

Figure S3

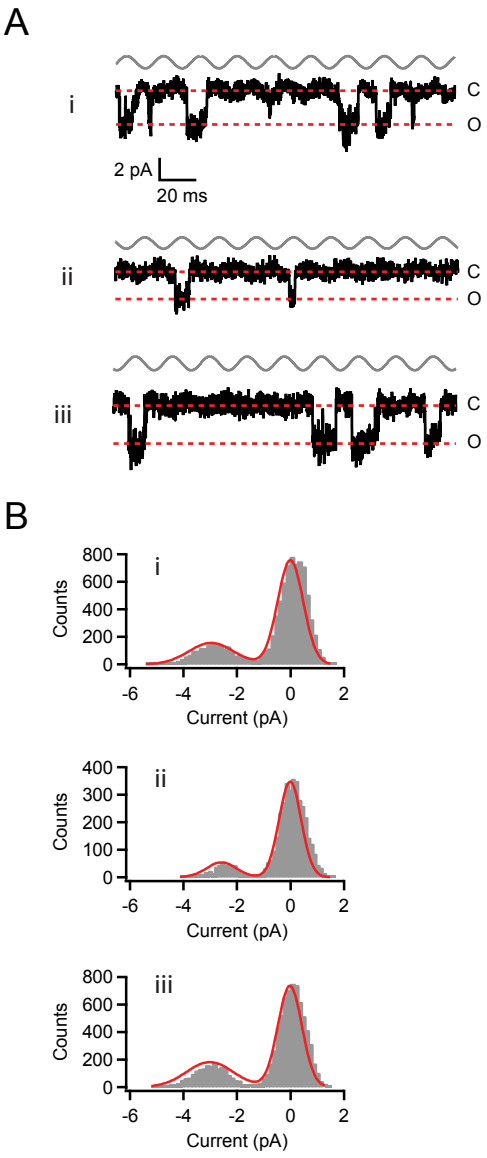
A
i
C
O
2 pA
20 ms
ii
C
O
iii
C
O
B
i
Counts
800
600
400
200
0
-6
-4
-2
0
2
Current (pA)
ii
Counts
400
300
200
100
0
-6
-4
-2
0
2
Current (pA)
iii
Counts
800
600
400
200
0
-6
-4
-2
0
2
Current (pA)

Figure S3: Piezo1 single channel currents during repetitive stimulation. Related to Figure 1.

(A) Stimulus protocol (gray) and representative single-channel currents (black) during the last second of a four second, 50 Hz sinusoidal stimulus. Red dashed lines indicate closed and open current amplitudes. Current traces are from N = 3 cells. (B) Calculated amplitude histograms from patches in (A). Single-channel current amplitudes were measured for 2-5 openings and calculated from multi-peak Gaussian analysis (IgorPro) of current amplitude histograms (red lines). Unitary conductance was then calculated using the holding potential of −80 mV.

Figure S4

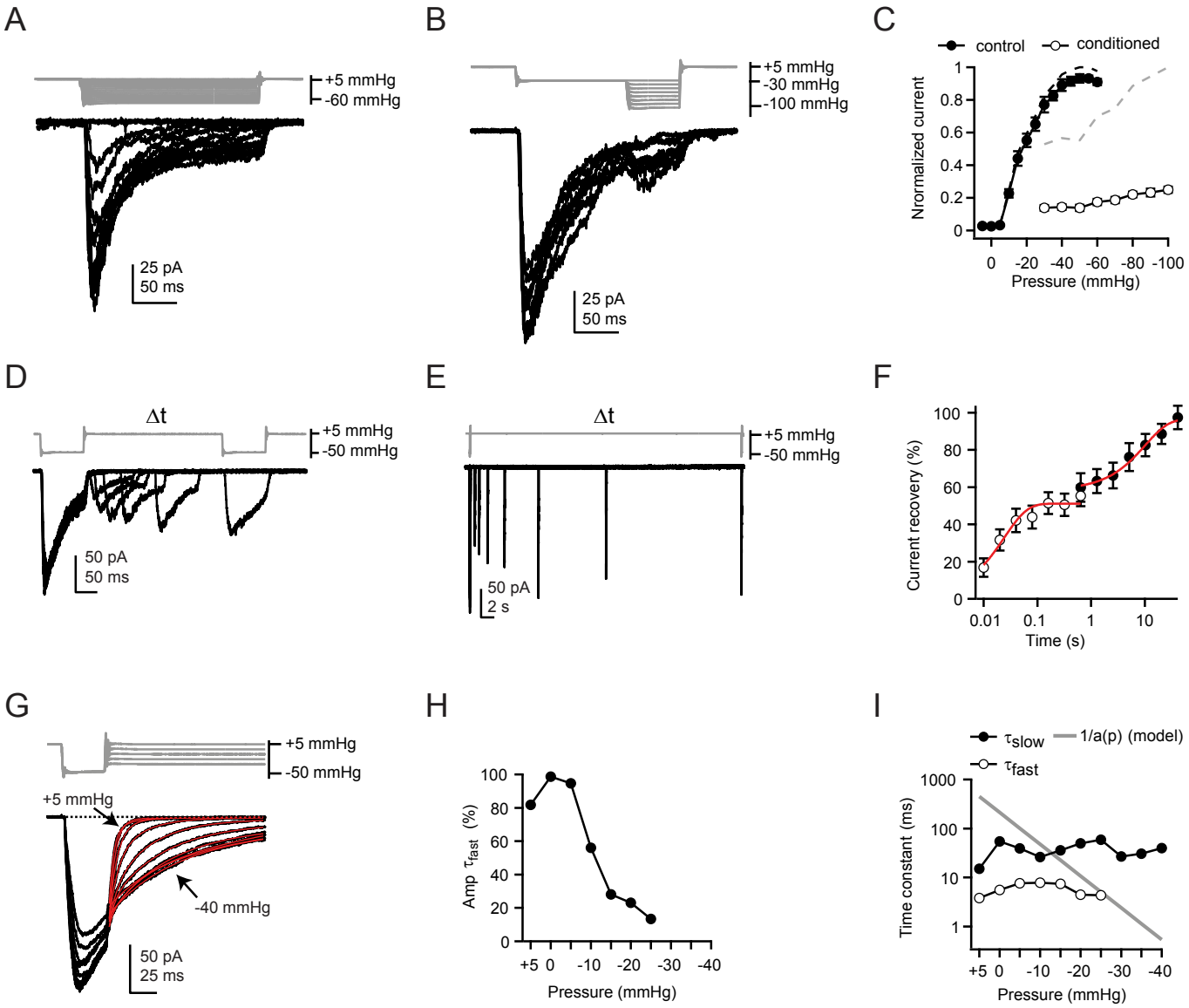
A
+5 mmHg
-60 mmHg
25 pA
50 ms
B
+5 mmHg
-30 mmHg
-100 mmHg
25 pA
50 ms
C
control
conditioned
Nrormalized current
Pressure (mmHg)
D
Δt
+5 mmHg
-50 mmHg
50 pA
50 ms
E
Δt
+5 mmHg
-50 mmHg
50 pA
2 s
F
Current recovery (%)
Time (s)
G
+5 mmHg
-50 mmHg
+5 mmHg
-40 mmHg
50 pA
25 ms
H
Amp τfast (%)
Pressure (mmHg)
I
τslow
1/a(p) (model)
τfast
Time constant (ms)
Pressure (mmHg)

Figure S4: Kinetic properties of Piezo1 inactivation and deactivation. Related to Figure 4.

(A) Stimulus protocol (gray) and representative currents (black) from a cell-attached patch from a HEK293t cell transiently expressing mouse Piezo1 in response to a standard pressure step protocol. (B) Stimulus protocol (gray) and representative currents (black) in response to an adaptation protocol in which patches are first conditioned by a 125 ms step to -30 mmHg to inactivate current before applying a standard pressure step protocol. (C) Mean pressure-evoked current amplitudes using the protocols in (A) (control, closed circles) and (B) (conditioned, open circles). For control cells, currents were normalized to the maximum response from that cell; for conditioned cells, currents were normalized to a single step pulse to -60 mmHg (not shown). Conditioned data are renormalized (dashed gray line) for comparison of pressure-dependence. N=11, control; N=11, conditioned. (D) and (E) Two step recovery stimulus protocol (gray) and representative currents (black) from a HEK293t cell transiently expressing mouse Piezo1. Protocol was split into short (D) and long (E) components to ensure patch integrity throughout the protocol. (F) Mean current recovery, calculated as peak current during the second pulse minus steady-state current at the end of the first pulse, normalized to the peak of the first pulse. Short (open circles) and long (closed circles) recovery courses were fit separately with single exponentials ($y = A*\exp(x/\tau)$) of 24 ms and 10.2 s, respectively. N = 16 cells (short); N = 12 cells (long). (G) Stimulus protocol designed to measure pressure dependence of deactivation and inactivation (gray) and mean currents (black) from HEK293t cells transiently expressing mouse Piezo1. Currents were fit (red) with double exponentials of the form $y = A_{fast}*\exp(x/\tau_{fast}) + A_{slow}*\exp(x/\tau_{slow})$. (H) Amplitude of τ_{fast} from double exponential fits in (F), calculated as % $\tau_{fast} = A_{fast}/(A_{fast} + A_{slow})$. Error bars obscured by data points. (I) Time constants (τ_{fast} and τ_{slow}) from double exponential fits in (F) (black symbols) and 1/a(p) (gray line), calculated from pressure-dependent rate constant 'a' from a best-fit model of Piezo1 gating (**Figure 4**). N = 11 cells. All data are mean ± s.e.m.

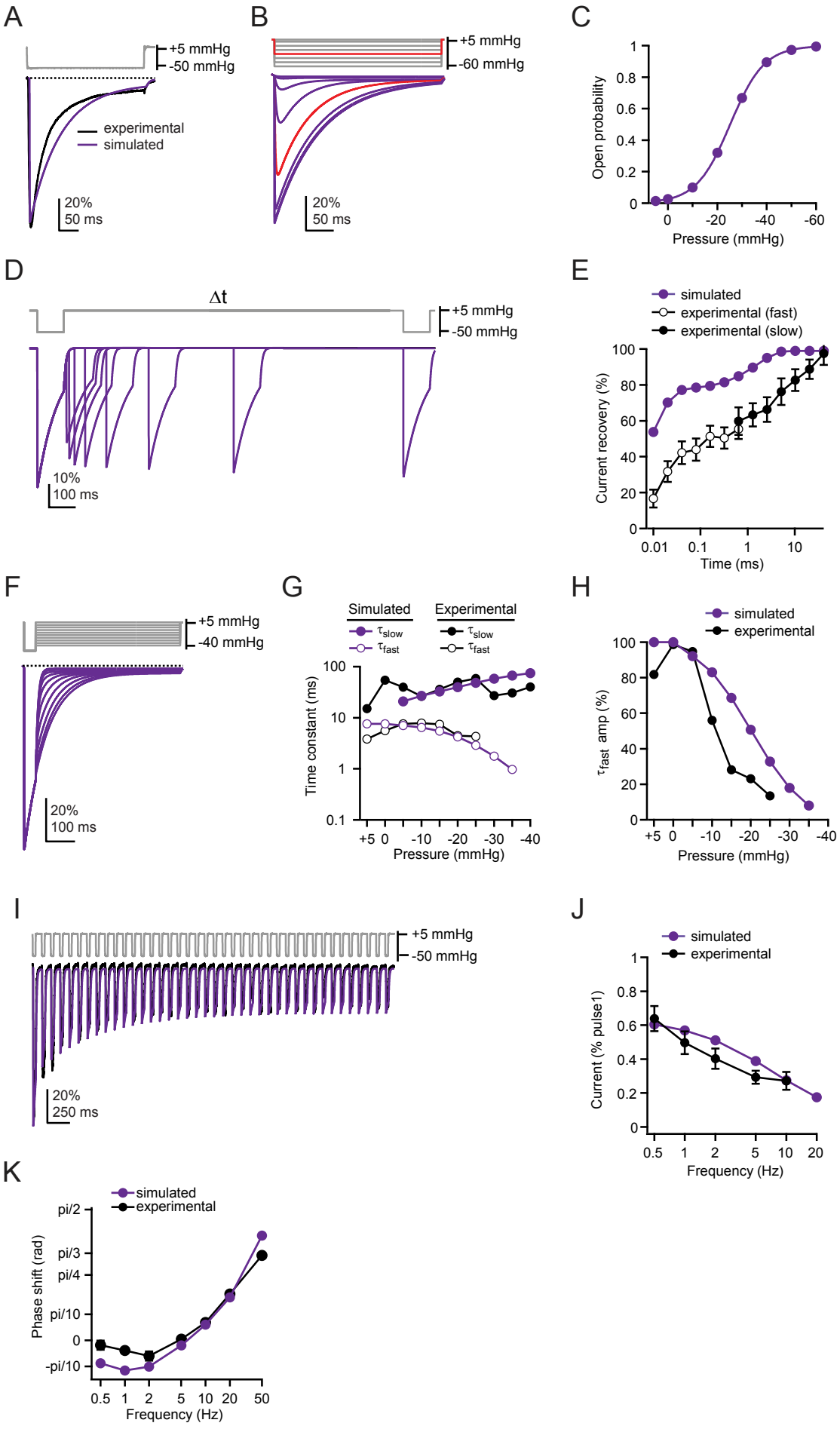
A
+5 mmHg
-50 mmHg
experimental
simulated
20%
50 ms
B
+5 mmHg
-60 mmHg
20%
50 ms
C
Open probability
Pressure (mmHg)
D
Δt
+5 mmHg
-50 mmHg
10%
100 ms
E
simulated
experimental (fast)
experimental (slow)
Current recovery (%)
Time (ms)
F
+5 mmHg
-40 mmHg
20%
100 ms
G
Simulated
Experimental
τslow
τfast
Time constant (ms)
Pressure (mmHg)
H
simulated
experimental
τfast amp (%)
Pressure (mmHg)
I
+5 mmHg
-50 mmHg
20%
250 ms
J
simulated
experimental
Current (% pulse1)
Frequency (Hz)
K
simulated
experimental
Phase shift (rad)
pi/2
pi/3
pi/4
pi/10
0
-pi/10
Frequency (Hz)

Figure S5: Piezo1 model recapitulates basic kinetic gating properties. Related to Figures 3 and 4.

(A) Stimulus protocol (gray), normalized and averaged experimental currents from HEK293t cells transiently transfected with Piezo1 elicited by a 300 ms negative pressure step (‘*step1’*; see **Figure 1C**) (black), and simulated currents using the best fit to the model in (A) (purple). Dashed gray line represents zero current. (B) Stimulus protocol (gray) and simulated currents (black) in response to a series of 300 ms pressure steps from +5 mmHg to -60 mmHg. Red protocol and current trace are -30 mmHg step. (C) Open probability as a function of pressure for simulated currents in (B); response curve is fit with a Boltzmann function (red line): $I = I_{max}/(1+\exp(-(P-P_{50})/k)$ where I_{max} is the maximal open probability, P is pressure, P_{50} is pressure of half-maximal activation, and k is the slope factor. Fit parameters I_{max} = 1.0, P_{50} = -25.2 mmHg, k = 6.9 mmHg. (D) Two pulse recovery protocol (gray) and simulated currents (black) (see **Figure S4C-E**). (E) Mean current recovery, calculated as peak current during the second pulse minus steady-state current at the end of the first pulse, normalized to the peak of the first pulse, for simulated currents (purple) and experimental data (black). N = 16 cells (short); N = 12 cells (long). Simulated data were fit with a double exponential ($y = A_{fast}*\exp(x/\tau_{fast}) + A_{slow}*\exp(x/\tau_{slow})$) and yielded τ_{fast} = 8.5 ms and τ_{slow} = 1.5 s. (F) Stimulus protocol designed to measure pressure dependence of deactivation and inactivation (gray) and simulated currents (black) (see **Figure S4F-H**). (G) Time constants (τ_{fast} and τ_{slow}) from a double exponential fit to simulated currents in (F) (purple) and to experimental data (black). N = 11 cells. (H) Amplitude of τ_{fast} from fits in (F), calculated as % $\tau_{fast} = A_{fast}/(A_{fast} + A_{slow})$. (I) Stimulus protocol (gray), normalized and averaged experimental currents elicited by a 10 Hz square pressure stimulus (see **Figure 3**) (black) and corresponding simulated currents (purple). Dashed line represents zero current. (J) Mean amplitudes of the ‘*last peak*’ currents for simulated (purple) and experimental (black) data, normalized to the peak amplitude of ‘*step1’* for each frequency. N = 7-11 cells per frequency. (K) Phase shift of currents relative to pressure stimulus for the last 2 s of stimulation for simulated (purple) and experimental (black) data. Error bars are obscured by data points. All data are mean ± s.e.m.

Supplemental Experimental Procedures

Electrophysiology

Patch-clamp recordings were performed at room temperature using an EPC10 amplifier and Patchmaster software (HEKA Elektronik, Lambrecht, Germany). Data were sampled at 5 kHz (cell-attached) or 10 kHz (whole-cell) and filtered at 2.9 kHz.

For whole-cell experiments, borosilicate glass pipettes (1.5 OD, 0.85 ID; Sutter Instrument Company, Novato, CA) had a resistance of 3-6 MΩ when filled with pipette buffer solution (voltage-clamp, in mM: 133 CsCl, 10 HEPES, 1 EGTA, 2 MgCl2, 4 MgATP, 0.4 Na2GTP, pH 7.3 with CsOH; current-clamp, in mM: 140 KCl, 0.5 EGTA, 5 HEPES, 3 Na2ATP, pH 7.3 with KOH). The bath solution for all whole-cell experiments was 130 NaCl, 3 KCl, 1 MgCl2, 10 HEPES, 2.5 CaCl2, 10 glucose (pH 7.3 with NaOH). Cells were held at -100 mV (HEK293t) or -80 mV (DRG). For whole-cell recordings, internal solution was allowed to dialyze for at least five minutes before recording to allow for GTP-mediated run-up of Piezo2 currents (Jia et al., 2013). Series resistance was compensated by 30-70%. Voltages were not corrected for a liquid junction potential.

For cell-attached experiments, pipettes had a resistance of 1.5-4 mΩ when filled with pipette buffer solution (in mM: 130 NaCl, 5 KCl, 10 HEPES, 10 TEACl, 1 CaCl2, 1 MgCl2, pH 7.3 with NaOH). The cell-attached bath solution used to zero the membrane potential was (in mM): 140 KCl, 10 HEPES, 1 MgCl2, 10 glucose, pH 7.3 with KOH. Patches were held at -80 mV except where described otherwise.

Cell Culture

For whole-cell experiments, cells were transiently transfected with Fugene6 (Promega, Madison, WI) in 6-well plates in the presence of 10 μM ruthenium red with wild-type or mutant mouse Piezo2 (2 μg) and GFP (1 μg) ~48 hours before recording. Transfected cells were reseeded at low density ~24 hours before recording onto glass coverslips coated with poly-L-lysine and laminin. For cell-attached experiments, cells were directly plated on coverslips and transfected with mouse Piezo1-pIRES-EGFP (1.5 μg) or co-transfected with pcDNA3.1(+) (empty vector; 1 μg) and GFP (0.5 μg) 24-48 hours before recording, as described above.

Mechanical Stimulation

In cell-attached patches, negative pressure was applied through the patch pipette with an amplifier-controlled high-speed pressure clamp system (HSPC-1; ALA Scientific Instruments, Farmingdale, NY). The rise time achieved by the pressure clamp for a direct step from +5 mmHg to -50 mmHg was ~2 ms. The maximal sinusoidal frequency achieved without undershooting commanded pressure was 20 Hz; at 50 Hz, the pressure measured oscillated from ~ +3.75 mmHg to -48.5 mmHg. In all figures, the stimulus protocol displayed is the pressure recorded, not the voltage command to the device. Prior to applying sinusoidal stimulation protocols, negative pressure steps (500 ms; in increasing -10 mmHg increments) were applied to each patch to assess initial current density. Sinusoidal waveforms were generated in PatchMaster; to phase-shift the stimulation, the first portion of the stimulus was a linear ramp with a duration of $\pi/2$. Square waveforms were applied for 30 ms, with a 3 ms on-ramp and 2 ms off-ramp to minimize pressure oscillations.

For whole-cell experiments, cells were indented with a fire-polished glass pipette (tip diameter ~3-5 μm) by an amplifier-controlled piezo-electric driver (E625 LVPZT Controller/Amplifier; Physik Instrumente) operated in closed-loop mode. The probe was initially positioned ~2-4 μm from the cell and advanced at 0.5 μm/ms in 1 μm increments at an 80° angle and square waveforms were applied for 10 ms; retractions were a 10 ms ramp (1-20 Hz) or 5 ms ramp (40 Hz) to prevent cell damage. In all figures, the stimulus protocol displayed is the distance actually travelled by the probe, not the voltage command to the device. The maximum frequency routinely achievable was 40 Hz (assuming a maximum indentation of 20 μm (10 ms on ramp, 10 ms stimulus, 5 ms off-ramp)). All indentation depths indicate distances beyond the first step at which the probe made visible contact with the cell (= 0 μm). The largest indentation depth in which the recording remained stable at all frequencies was used for analysis. Unless

stated otherwise, all mechanical stimulation was preceded (‘*step1*‘) and followed (‘*step2*’) by single test pulses that were separated from stimuli by 10 seconds at 0 μm (whole-cell) or +5 mmHg (cell-attached) and sweeps were separated by 10 seconds to allow for recovery from inactivation.

Gating model of Piezo1

Currents were simulated using acquired pressure traces and compared to mean current traces experimentally acquired at -80 mV at 2, 5, 10, and 20 Hz (normalized to the peak current of ‘*step1’* for each cell); 0.5 Hz and 1 Hz were not used because the small currents lead to greater errors in the fit and 50 Hz was not used because the pressure clamp was operating at the upper limit of its speed and slightly undershot maximum pressure values. Although the stimulus sensed by Piezo1 is tension, not pressure (Lewis and Grandl, 2015; Cox et al., 2016), here, we used a narrow size of pipette ranges (i.e., radii) such that the tension-pressure relationship is consistent among patches. Initial values for rate constants a, b, and c were estimated from a bi-exponential fit to a single step to -50 mmHg (0.0025 ms^{-1}, 0.015 ms^{-1}, and 0.027 ms^{-1}, respectively) and the slope (k) (such that $a(p) = a_0 \cdot \exp(-p/k)$ and $e(p) = e_0 \cdot \exp(p/k)$) was initially set to 10 mmHg. We assumed pressure-dependent rate constants for a(p) and e(p) based on previous models for Piezo1 (Gottlieb et al., 2012; Bae et al., 2013) as well as our own data showing pressure-independence for b (**Figure S4**); we assumed pressure-independence for f, as this would unilaterally reduce availability of channels without significantly affecting the profile of evoked currents. Initial estimated values for rate constants e and h were taken from two pulse recovery experiments (.0035 ms^{-1} and .00015 ms^{-1}, respectively; **Figure S4**). Initial estimated values for rate constants d, f, and g (0.0015 ms^{-1}, 0.0001 ms^{-1}, and 0.0027 ms^{-1}) were then varied combinatorically by a factor of 0.1 and 10, with either d or f being dependent on the other values to obey microscopic reversibility (a*c*e = b*d*f). We also incorporated a delay constant to account for a potential time delay between pressure measured at the piezoelectric valve in the pressure clamp headstage and transmission of tension to the channel, and this was initially set to 0 ms. This gave 18 different combinations of initial rate constants; we initially allowed the second inactivated state (I_2) to arise from either the first inactivated state or from the open state, for a total of 36 initial inputs. From each initial set of input values, each rate constant was iteratively varied ±1% in 0.1% increments and the value minimizing the residual between real and simulated data was used for the next iteration until rate constants stabilized. 17 of 18 initial solutions found the same general set of rate constants for each possible location of I_2, with no differences greater than 2-fold in any given rate constant. For these 36 initial “solutions”, the global residual was then calculated for all 7 frequencies (0.5, 1, 2, 5, 10, 20, and 50 Hz) to identify the final best fit, which arose from a solution modeling I_2 entry from O and had a global residual of 1.9%; the lowest residual modeling I_2 entry from I_1 was 2.0%. The delay constant for the best fit solution was 6.4 ms. To ensure that the model was not unfairly biased by the initial inputs for a, b, c, e, and h, we ran a final set of 10 inputs in which the values for each constant (a, b, c, e, and h) were changed by a factor of 0.1 and 10, with values for d, f, and g taken from the input values that gave the best solution in the previous round; all 10 found the same general solution as before.

Supplemental References

Bae C, Gnanasambandam R, Nicolai C, Sachs F, Gottlieb PA (2013) Xerocytosis is caused by mutations that alter the kinetics of the mechanosensitive channel PIEZO1. Proceedings of the National Academy of Sciences of the United States of America 110:E1162-1168.

Cox CD, Bae C, Ziegler L, Hartley S, Nikolova-Krstevski V, Rohde PR, Ng CA, Sachs F, Gottlieb PA, Martinac B (2016) Removal of the mechanoprotective influence of the cytoskeleton reveals PIEZO1 is gated by bilayer tension. Nat Commun 7:10366.

Gottlieb PA, Bae C, Sachs F (2012) Gating the mechanical channel Piezo1: a comparison between whole-cell and patch recording. Channels (Austin) 6:282-289.

Lewis AH, Grandl J (2015) Mechanical sensitivity of Piezo1 ion channels can be tuned by cellular membrane tension. eLife 4.

Wu J, Goyal R, Grandl J (2016) Localized force application reveals mechanically sensitive domains of Piezo1. Nat Commun 7:12939.